

Missing dust signature in the cosmic microwave background

Václav Vavryčuk,¹★

¹*Institute of Geophysics, The Czech Academy of Sciences, Boční II, Praha 4, 14100, Czech Republic*

Accepted May 4, 2017. Received April 29, 2017; in original form March 5, 2017

ABSTRACT

I examine a possible spectral distortion of the Cosmic Microwave Background (CMB) due to its absorption by galactic and intergalactic dust. I show that even subtle intergalactic opacity of $1 \times 10^{-7} \text{ mag } h \text{ Gpc}^{-1}$ at the CMB wavelengths in the local Universe causes non-negligible CMB absorption and decline of the CMB intensity because the opacity steeply increases with redshift. The CMB should be distorted even during the epoch of the Universe defined by redshifts $z < 10$. For this epoch, the maximum spectral distortion of the CMB is at least $20 \times 10^{-22} \text{ Wm}^{-2} \text{ Hz}^{-1} \text{ sr}^{-1}$ at 300 GHz being well above the sensitivity of the COBE/FIRAS, WMAP or Planck flux measurements. If dust mass is considered to be redshift dependent with noticeable dust abundance at redshifts 2–4, the predicted CMB distortion is even higher. The CMB would be distorted also in a perfectly transparent universe due to dust in galaxies but this effect is lower by one order than that due to intergalactic opacity. The fact that the distortion of the CMB by dust is not observed is intriguing and questions either opacity and extinction law measurements or validity of the current model of the Universe.

Key words: cosmic background radiation – dust, extinction – early Universe – galaxies: high redshift – galaxies: ISM – intergalactic medium

1 INTRODUCTION

Observations of the Cosmic Microwave Background (CMB) based on rocket measurements of Gush et al. (1990) and FIRAS on the COBE satellite (Mather et al. 1990; Fixsen et al. 1996) proved that the CMB has almost a perfect thermal black-body spectrum with an average temperature of $T = 2.728 \pm 0.004 \text{ K}$ (Fixsen et al. 1996). The accuracy was improved using the WMAP data, which yielded an average temperature of $T = 2.72548 \pm 0.00057 \text{ K}$ (Fixsen 2009). Observed tiny large-scale variations of the CMB temperature of $\pm 0.00335 \text{ K}$ are attributed to the motion (including rotation) of the Milky Way relative to the Universe (Kogut et al. 1993). The small-scale variations of $\pm 300 \mu\text{K}$ traced, for example, by the WMAP (Bennett et al. 2003; Hinshaw et al. 2009; Bennett et al. 2013), ACBAR (Reichardt et al. 2009), and BOOMERANG (MacTavish et al. 2006) instruments using angular multipole moments are attributed to basic properties of the Universe as its curvature or the dark-matter density (Spergel et al. 2007; Komatsu et al. 2011).

Since the CMB as a relic radiation of the Big Bang experienced different epochs of the Universe, it interacted with matter of varying physical and chemical properties.

Distortions of the CMB due to this interaction comprise the μ -type (at $z \gtrsim 10^5$) and y -type (at $z \lesssim 10^4$) distortions related to the photon-electron interactions, distortions produced by the reionized IGM, and presence of galactic and extragalactic foregrounds (Wright 1981; Chluba & Sunyaev 2012; De Zotti et al. 2016). The foreground contamination of the CMB due to diffuse emission of intergalactic dust thermalized by absorption of starlight was estimated, for example, by Imara & Loeb (2016b). They found that the predicted contamination is under the detection of the COBE/FIRAS experiments (Mather et al. 1994; Fixsen et al. 1996) but it should be recognized in observations of the Primordial Inflation Explorer (PIXIE; Kogut et al. 2014) and the Polarized Radiation Imaging and Spectroscopy Mission (PRISM; André et al. 2014) that would exceed the spectral sensitivity limits of COBE/FIRAS by 3–4 orders of magnitude.

Another possible origin of distortion of the CMB related to galactic and intergalactic dust is absorption of the CMB by dust. Absorbing properties of dust grains have been discussed by Wright (1987, 1991); Henning et al. (1995); Stognienko et al. (1995) and others, who pointed out that the long-wavelength absorption of needle-shaped conducting grains or complex fractal or fluffy dust aggregates might provide a sufficient opacity for the CMB. Hence, it is worth to model the CMB attenuation by dust and to check if is de-

★ E-mail: vv@ig.cas.cz

tectable or not. In this paper, I study the spectral and total distortions of the CMB due to absorption by dust. I find that the imprint of cosmic dust in the CMB predicted by theory is not negligible; however, it is missing in observations even though it is above their current detection level.

2 THEORY

2.1 Optical depth

Effective optical depth $\tau(z)$ for light emitted at redshift z is expressed as [Peebles \(1993, his equation 13.42\)](#)

$$\tau(z) = \int_0^z n_D \sigma (1+z')^2 \frac{c}{H_0} \frac{dz'}{E(z')}, \quad (1)$$

where n_D is the comoving dust number density, σ is the attenuation cross-section, $E(z)$ is the dimensionless Hubble parameter

$$E(z) = \sqrt{(1+z)^2 (1 + \Omega_m z) - z(2+z)\Omega_\Lambda}, \quad (2)$$

c is the speed of light, H_0 is the Hubble constant, Ω_m is the total matter density, Ω_Λ is the dimensionless cosmological constant.

Eq. (1) can be rewritten using galactic and intergalactic attenuation coefficients ε^G and ε^{IG} as

$$\tau(z) = \frac{c}{H_0} \int_0^z (\varepsilon^G + \varepsilon^{IG}) (1+z')^2 \frac{dz'}{E(z')}, \quad (3)$$

where

$$\varepsilon^G = \frac{\kappa}{\gamma}, \quad (4)$$

κ is the mean galactic opacity, γ is the mean free path of a light ray between galaxies in the comoving space

$$\gamma(z) = \frac{1}{n\pi a^2}, \quad (5)$$

a is the mean galaxy radius, and n is the galaxy number density in the comoving space. Eq. (3) is valid for frequency-independent attenuation. Considering the ' $\lambda^{-\beta}$ extinction law', where λ is the wavelength of light ([Mathis 1990; Calzetti et al. 1994; Charlot & Fall 2000; Draine 2003](#)), we can express the galactic and intergalactic attenuations at frequency ν using the reference quantities related to observed frequency ν_0 ,

$$\varepsilon_\nu^G = \nu^\beta \varepsilon_0^G, \quad \varepsilon_\nu^{IG} = \nu^\beta \varepsilon_0^{IG}. \quad (6)$$

Eq. (3) is then modified to

$$\tau_\nu(z) = \frac{c}{H_0} \left(\frac{\nu}{\nu_0} \right)^\beta \int_0^z (\varepsilon_0^G + \varepsilon_0^{IG}) (1+z')^{2+\beta} \frac{dz'}{E(z')}, \quad (7)$$

expressing the fact that light is more attenuated at high z because of its shift to high frequencies.

2.2 Extinction of the CMB

Assuming the CMB to be a perfect blackbody radiation, its spectral intensity (i.e., energy received per unit area from a unit solid angle in the frequency interval ν to $\nu + d\nu$, in $\text{Wm}^{-2} \text{Hz}^{-1} \text{sr}^{-1}$) is described by the Planck's law

$$I_\nu = \frac{2h\nu^3}{c^2} \frac{1}{e^{h\nu/k_B T_{\text{CMB}}} - 1}, \quad (8)$$

where ν is the frequency, T_{CMB} is the CMB temperature, h is the Planck constant, c is the speed of light, and k_B is the Boltzmann constant. Since the CMB is attenuated by galactic and intergalactic opacity, we can evaluate the distortion of the spectral CMB intensity at frequency ν along light ray coming from redshift z as

$$\Delta I_\nu(z) = I_\nu \left(1 - e^{-\tau_\nu(z)} \right), \quad (9)$$

where τ_ν and I_ν are defined in eqs (7) and (8). Consequently, the reduction of the total CMB intensity (in $\text{Wm}^{-2} \text{sr}^{-1}$) is

$$\Delta I(z) = \int \Delta I_\nu d\nu. \quad (10)$$

Evaluating eqs (9) and (10) for different redshifts z , we can predict the distortion of the CMB intensity by the opacity of the Universe when going back in cosmic time up to redshift z . Such approach is advantageous because it suppresses uncertainties in observed parameters needed in calculations. We start at present time, when the galactic and intergalactic opacities are best constrained from observations, and gradually extrapolate the prediction to higher redshifts.

3 OPACITY OBSERVATIONS

In order to evaluate the CMB distortion due to absorption by dust, we need estimates of the dust mass in the Universe and its history. The most straightforward way is to use observations of the galactic and intergalactic opacities at visual wavelengths mapping the distribution of dust in galaxies and intergalactic space and relate the visual and CMB opacities using the extinction law describing the dependence of attenuation of light on wavelength.

3.1 Galactic and intergalactic opacities

The opacity of galaxies depends basically on their type and age (for a review, see [Calzetti, 2001](#)). The most transparent galaxies are elliptical with an effective extinction A_V of 0.04 – 0.08 mag. The light extinction by dust in spiral and irregular galaxies is higher ([González et al. 1998; Holwerda et al. 2005b,a, 2013; Holwerda & Keel 2013](#)). Typical values for the inclination-averaged extinction are: 0.5 – 0.75 mag for Sa-Sab galaxies, 0.65 – 0.95 mag for the Sb-Scd galaxies, and 0.3 – 0.4 mag for the irregular galaxies at the B-band ([Calzetti 2001](#)). Considering the relative frequency of galaxy types in the Universe, we can average the visual extinctions of individual galaxy types and calculate the mean visual extinction and the mean visual galactic opacity. According to [Vavryčuk \(2017\)](#), the average value of visual opacity κ_V is about 0.22 ± 0.08 at $z = 0$.

The intergalactic opacity is lower by several orders than the galactic opacity being observed, particularly, in galaxy halos and in cluster centres ([Ménard et al. 2010a](#)). The opacity in the galaxy clusters has been measured by reddening of background objects behind the clusters ([Chelouche et al. 2007; Bovy et al. 2008; Muller et al. 2008](#)). The intergalactic opacity can also be measured by correlations between the positions of low-redshift galaxies and high-redshift QSOs. [Ménard et al. \(2010a\)](#) correlated the brightness of $\sim 85,000$ quasars at $z > 1$ with the position of 24 million galaxies at $z \sim 0.3$ derived from the SDSS. The estimated value of A_V

is about 0.03 mag at $z = 0.5$ and about 0.05 – 0.09 mag at $z = 1$. A consistent opacity is reported by Xie et al. (2015) who investigated the redshifts and luminosity of the quasar continuum of $\sim 90,000$ objects. The authors estimated the visual opacity to be $\sim 0.02 h \text{ Gpc}^{-1}$ at $z < 1.5$. As mentioned by Ménard et al. (2010b) such opacity is not negligible and can lead to bias in determining cosmological parameters if ignored.

3.2 Evolution of opacity with redshift

The galactic and intergalactic opacities depend on redshift. First, they increase with redshift due to the expansion of the Universe. This geometrical effect has already been taken into account in eq. (1) by considering an increasing dust density with redshift because the Universe occupied a smaller volume in its early epoch. Second, a redshift-dependent formation and evolution of global dust mass in galaxies and in intergalactic space must be taken into account.

Observations indicate that interstellar dust mass M_d is strongly linked to the star formation rate (SFR) of galaxies. da Cunha et al. (2010) analysed 3258 low-redshift SDSS galaxies with $z < 0.2$ and reported the relation $M_d \sim \text{SFR}^{1.1}$. Calura et al. (2017) extended the dataset with high-redshift galaxies from Santini et al. (2010) and found a similar relation with a slightly lower slope of ~ 0.9 . The same slope is reported also by Hjorth et al. (2014). Adopting the M_d –SFR relation, we deduce from the SFR history (see Fig. 1) that the global dust mass steeply increases for $z < 2 - 2.5$, it culminates at $z = 3 - 4$ and then it starts to decline (Madau et al. 1996; Hopkins & Beacom 2006; Madau & Dickinson 2014; Popping et al. 2016). The decline is not, however, substantially steep because dust is reported even in star-forming galaxies at redshifts of $z > 5$ (Casey et al. 2014). Based on observations of the Atacama Large Millimeter Array (ALMA), Watson et al. (2015) investigated a galaxy at $z > 7$ highly evolved with a large stellar mass and heavily enriched in dust. Similarly, Laporte et al. (2017) analysed a galaxy at a photometric redshift of $z \sim 8$ with a stellar mass of $\sim 2 \times 10^9 M_\odot$, a SFR of $\sim 20 M_\odot \text{ yr}^{-1}$ and a dust mass of $\sim 6 \times 10^6 M_\odot$.

3.3 Extinction law

The light extinction due to absorption by dust is frequency dependent (see Fig. 2). In general, it decreases with increasing wavelength but displays irregularities. The extinction curve for dust in the Milky Way can be approximated for infrared wavelengths between $\sim 0.9 \mu\text{m}$ and $\sim 5 \mu\text{m}$ by a power-law $A_\lambda \sim \lambda^{-\beta}$ with β ranging between 1.61 and 1.81 (Draine 2003, 2011). At wavelengths of 9.7 and $18 \mu\text{m}$, the absorption displays two distinct maxima attributed to silicates (Mathis 1990; Li & Draine 2001; Draine 2003). At longer wavelengths, the extinction curve is smooth obeying a power-law with $\beta = 2$. This decay is also predicted by the Mie theory modelling graphite or silicate dust grains as small spheres or spheroids with sizes up to $1 \mu\text{m}$ (Draine & Lee 1984). However, Wright (1982); Henning et al. (1995); Stognienko et al. (1995) and others point out that the long-wavelength absorption also depends on the shape of the dust grains and that needle-shaped conducting grains or complex fractal or fluffy dust aggregates can provide higher

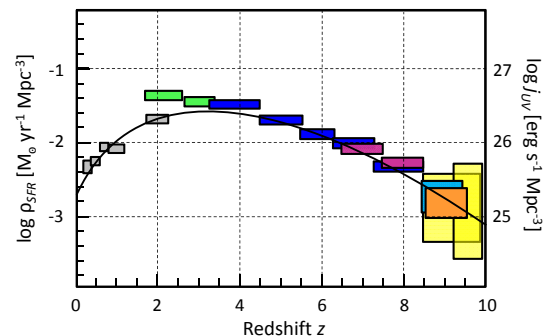


Figure 1. The SFR traced by the UV luminosity density as a function of redshift. Observations are taken from Schiminovich et al. (2005) (grey rectangles), Reddy & Steidel (2009) (green rectangles), Bouwens et al. (2014a) (blue rectangles), McLure et al. (2013) (magenta rectangles), Ellis et al. (2013) (orange rectangle), Oesch et al. (2014) (light blue rectangle), and Bouwens et al. (2014b) (yellow rectangles). The solid black line reproduces the SFR evolution used in the modelling of evolution of dust mass.

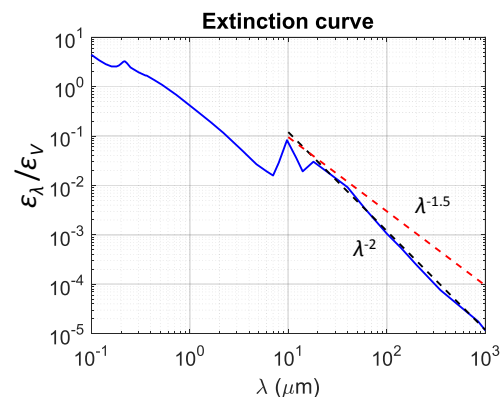


Figure 2. Normalized frequency-dependent attenuation (Draine 2003, his Tables 4-6). The black and red dashed lines show the long-wavelength asymptotic behaviour predicted by the power law with $\beta = 2$ and $\beta = 1.5$.

long-wavelength opacity with the power-law described by $0.6 < \beta < 1.4$ (Wright 1987).

4 PREDICTED CMB DISTORTION

I consider the intergalactic opacity at visual wavelengths of $0.01 \text{ mag } h \text{ Gpc}^{-1}$ that is a twice lower value than that reported by Xie et al. (2015). The ratio of the CMB and visual attenuation $\epsilon_{\text{CMB}}/\epsilon_V$ of 1×10^{-5} is taken from Mathis (1990) and Draine (2003). Actually, this ratio is very low being obtained for a steep decrease of attenuation at long wavelengths ($\beta = 2$). Realistic values for dust particles with complex shapes might be higher by one order (Wright 1987, $\beta = 1.5$). I intentionally use the low value of ϵ_{CMB} in order to be sure that the predicted level of the CMB distortion is the lower threshold of expected values.

The CMB distortion is calculated for two models. Model A is based on an assumption that the comoving dust density is independent of redshift. Model B adopts an interstellar and intergalactic dust density evolving with redshift in accordance with the SFR (see Fig. 1). The spectral and total

Table 1. Input parameters for modelling

a (kpc)	n ($h^3 \text{ Mpc}^{-3}$)	γ ($h \text{ Gpc}^{-1}$)	κ_V	β	ϵ_V^G ($h \text{ Gpc}^{-1}$)	ϵ_V^{IG} ($h \text{ Gpc}^{-1}$)	$\epsilon_{\text{CMB}}/\epsilon_V$	ϵ_{CMB}^G ($h \text{ Gpc}^{-1}$)	$\epsilon_{\text{CMB}}^{IG}$ ($h \text{ Gpc}^{-1}$)
10	0.02	160	0.22	2.0	1.4×10^{-3}	9.2×10^{-3}	1.0×10^{-5}	1.4×10^{-8}	9.2×10^{-8}

a is the mean effective radius of galaxies, n is the comoving number density of galaxies, γ is the mean free path between galaxies, κ_V is the mean visual opacity of galaxies, β is the slope in the extinction law, ϵ_V^G is the visual galactic attenuation coefficient defined in eq. (4), ϵ_V^{IG} is the visual intergalactic attenuation coefficient, ϵ_{CMB}^G and $\epsilon_{\text{CMB}}^{IG}$ are the galactic and intergalactic attenuation coefficients at the CMB wavelengths.

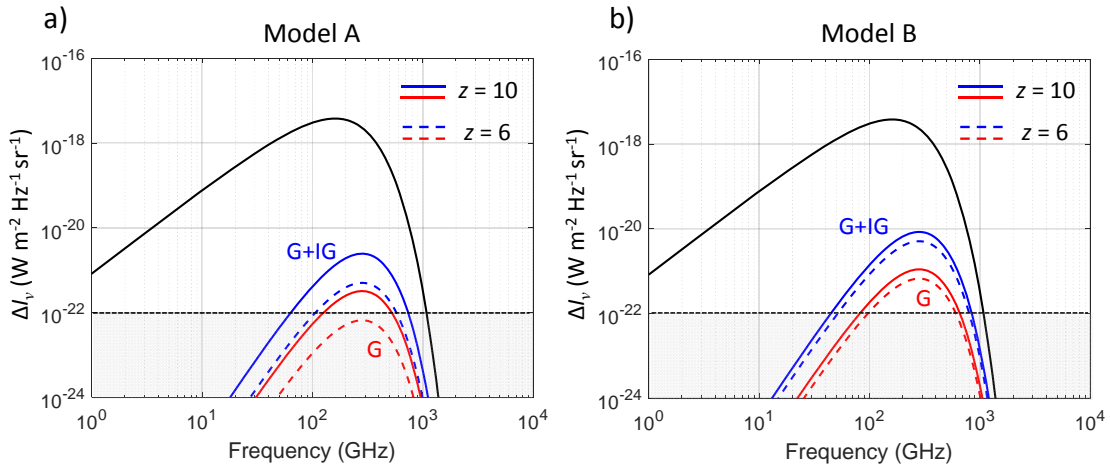


Figure 3. The spectral CMB distortion for Model A (a) and Model B (b). The full black line shows the spectral CMB intensity. Full blue/red lines - $z_{\text{max}} = 10$, dashed blue/red lines - $z_{\text{max}} = 6$. Blue lines - distortions due to galactic and intergalactic dust (G+IG), red lines - distortions due to galactic dust (G). The grey area marks intensities which are under the sensitivity of the COBE/FIRAS measurements at 300 GHz (Fixsen et al. 1996). Cosmological parameters: $H_0 = 70 \text{ km s}^{-1} \text{ Mpc}^{-1}$, $\Omega_m = 0.3$, and $\Omega_\Lambda = 0.7$.

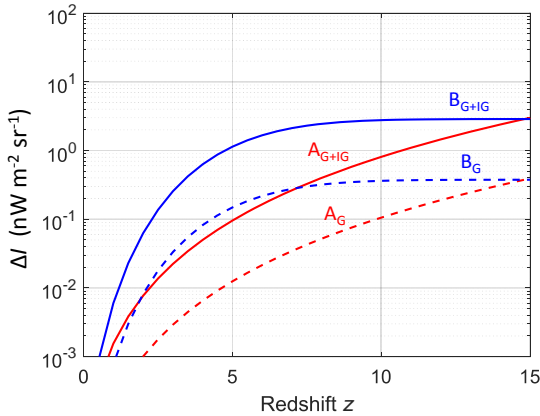


Figure 4. The total CMB distortion as a function of redshift for Model A (red) and Model B (blue). Full lines - distortions due to galactic and intergalactic dust (G+IG), dashed lines - distortions due to galactic dust (G).

CMB distortions are calculated using eqs (9) and (10) with parameters summarized in Table 1. In calculations, both of the galactic and intergalactic opacity (G+IG) or the galactic opacity only (G) are considered.

Fig. 3 shows the spectral CMB intensity and its corresponding distortion produced by dust in the epoch of

$0 < z < z_{\text{max}}$ with z_{max} of 6 and 10. As expected, the distortion increases with increasing z_{max} , but the effect of dust absorption is visible even for z_{max} of 6. The distortion is more pronounced for Model B than for Model A. This is caused by abundance of dust for $z \sim 2 - 4$ considered in Model B but neglected in Model A. The maximum distortion is observed at frequency of 300 GHz and reaches a value of $5.1 \times 10^{-22} \text{ W m}^{-2} \text{ Hz}^{-1} \text{ sr}^{-1}$ for Model A and $51.0 \times 10^{-22} \text{ W m}^{-2} \text{ Hz}^{-1} \text{ sr}^{-1}$ for Model B. These values exceed the detection level of the COBE/FIRAS (absolute sensitivity of $\sim 1 - 2 \times 10^{-22} \text{ W m}^{-2} \text{ Hz}^{-1} \text{ sr}^{-1}$, Fixsen et al. 1996) or WMAP and Planck flux measurements (absolute sensitivity of $\sim 7 \times 10^{-23} \text{ W m}^{-2} \text{ Hz}^{-1} \text{ sr}^{-1}$, Hinshaw et al. 2009; Planck Collaboration et al. 2014). The total CMB distortion is about 0.2 and $1.7 \text{ nW m}^{-2} \text{ sr}^{-1}$ for $z_{\text{max}} = 6$ for Model A and B, respectively (Fig. 4). Model B predicts a faster increase of the total CMB distortion with z_{max} than Model A. The maximum distortion increases up to $z_{\text{max}} \sim 7$. At higher z , the CMB is not distorted, because the model is effectively free of dust. Note that the reported values are the lower thresholds; the realistic distortions should be higher.

5 DISCUSSION

It is commonly considered that the CMB is distorted by foreground diffuse FIR and submillimetre emission of dust

in the Milky Way, other galaxies and intergalactic space (Draine & Fraise 2009; Imara & Loeb 2016b). However, the CMB can also be distorted due to absorption by dust producing a decline of the CMB intensity at all frequencies. This distortion should be high enough to be observable in the CMB measurements. The maximum spectral distortion of the CMB light coming from $z = 10$ is predicted at 300 GHz being at least 20 times higher than the detection level of the COBE/FIRAS measurements (Fixsen et al. 1996) and at least 35 times higher than the detection level of the WMAP or Planck measurements (Hinshaw et al. 2009; Planck Collaboration et al. 2014). The CMB should be distorted also in a perfectly transparent universe just due to absorption by dust in galaxies. This effect is about one order lower than that for the intergalactic opacity, but still above the detection level of the current CMB measurements.

Finally, let's shortly discuss why the imprint of dust is missing on the CMB. Firstly, we can speculate that the parameters used in modelling are seriously biased. However, it contradicts observations of the intergalactic opacity (Ménard et al. 2010a; Xie et al. 2015; Imara & Loeb 2016a), opacity of galaxies (González et al. 1998; Calzetti 2001; Holwerda et al. 2005b,a, 2013) and the extinction law data in the Milky Way (Draine & Lee 1984; Mathis 1990; Li & Draine 2001; Draine 2003). Secondly, we can question the Big Bang as the origin of the CMB and revive theory of the CMB as the thermal radiation of dust itself being produced at much later times than Big Bang (Layzer & Hively 1973; Wright 1982, 1987, 1991; Aguirre 2000). In such theory, the CMB should not be distorted because the CMB would concurrently be absorbed and reradiated by dust. In any case, it is clear that the missing dust imprint on the CMB is an intriguing puzzle which should be further studied and confronted with current measurements and models of the Universe.

ACKNOWLEDGEMENTS

I thank Benne W. Holwerda for his valuable comments which helped me to improve the quality of the paper.

REFERENCES

- Aguirre A. N., 2000, *ApJ*, **533**, 1
- André P., et al., 2014, *J. Cosmology Astropart. Phys.*, **2**, 006
- Bennett C. L., et al., 2003, *ApJS*, **148**, 1
- Bennett C. L., et al., 2013, *ApJS*, **208**, 20
- Bouwens R. J., et al., 2014a, *ApJ*, **793**, 115
- Bouwens R. J., et al., 2014b, *ApJ*, **795**, 126
- Bovy J., Hogg D. W., Moustakas J., 2008, *ApJ*, **688**, 198
- Calura F., et al., 2017, *MNRAS*, **465**, 54
- Calzetti D., 2001, *PASP*, **113**, 1449
- Calzetti D., Kinney A. L., Storchi-Bergmann T., 1994, *ApJ*, **429**, 582
- Casey C. M., Narayanan D., Cooray A., 2014, *Phys. Rep.*, **541**, 45
- Charlot S., Fall S. M., 2000, *ApJ*, **539**, 718
- Chelouche D., Koester B. P., Bowen D. V., 2007, *ApJ*, **671**, L97
- Chluba J., Sunyaev R. A., 2012, *MNRAS*, **419**, 1294
- da Cunha E., Eminian C., Charlot S., Blaizot J., 2010, *MNRAS*, **403**, 1894
- De Zotti G., Negrello M., Castex G., Lapi A., Bonato M., 2016, *J. Cosmology Astropart. Phys.*, **3**, 047
- Draine B. T., 2003, *ARA&A*, **41**, 241
- Draine B. T., 2011, *Physics of the Interstellar and Intergalactic Medium*
- Draine B. T., Fraise A. A., 2009, *ApJ*, **696**, 1
- Draine B. T., Lee H. M., 1984, *ApJ*, **285**, 89
- Ellis R. S., et al., 2013, *ApJ*, **763**, L7
- Fixsen D. J., 2009, *ApJ*, **707**, 916
- Fixsen D. J., Cheng E. S., Gales J. M., Mather J. C., Shafer R. A., Wright E. L., 1996, *ApJ*, **473**, 576
- González R. A., Allen R. J., Dirsch B., Ferguson H. C., Calzetti D., Panagia N., 1998, *ApJ*, **506**, 152
- Gush H. P., Halpern M., Wishnow E. H., 1990, *Physical Review Letters*, **65**, 537
- Henning T., Michel B., Stognienko R., 1995, *Planet. Space Sci.*, **43**, 1333
- Hinshaw G., et al., 2009, *ApJS*, **180**, 225
- Hjorth J., Gall C., Michałowski M. J., 2014, *ApJ*, **782**, L23
- Holwerda B. W., Keel W. C., 2013, *A&A*, **556**, A42
- Holwerda B. W., Gonzalez R. A., Allen R. J., van der Kruit P. C., 2005a, *AJ*, **129**, 1381
- Holwerda B. W., Gonzalez R. A., Allen R. J., van der Kruit P. C., 2005b, *AJ*, **129**, 1396
- Holwerda B. W., Böker T., Dalcanton J. J., Keel W. C., de Jong R. S., 2013, *MNRAS*, **433**, 47
- Hopkins A. M., Beacom J. F., 2006, *ApJ*, **651**, 142
- Imara N., Loeb A., 2016a, *ApJ*, **816**, L16
- Imara N., Loeb A., 2016b, *ApJ*, **825**, 130
- Kogut A., et al., 1993, *ApJ*, **419**, 1
- Kogut A., et al., 2014, in *Society of Photo-Optical Instrumentation Engineers (SPIE) Conference Series 9134*. p. 91431E, doi:10.1117/12.2056840
- Komatsu E., et al., 2011, *ApJS*, **192**, 18
- Laporte N., et al., 2017, *ApJ*, **837**, L21
- Layzer D., Hively R., 1973, *ApJ*, **179**, 361
- Li A., Draine B. T., 2001, *ApJ*, **554**, 778
- MacTavish C. J., et al., 2006, *ApJ*, **647**, 799
- Madau P., Dickinson M., 2014, *ARA&A*, **52**, 415
- Madau P., Ferguson H. C., Dickinson M. E., Gialavisco M., Steidel C. C., Fruchter A., 1996, *MNRAS*, **283**, 1388
- Mather J. C., et al., 1990, *ApJ*, **354**, L37
- Mather J. C., et al., 1994, *ApJ*, **420**, 439
- Mathis J. S., 1990, *ARA&A*, **28**, 37
- McLure R. J., et al., 2013, *MNRAS*, **432**, 2696
- Ménard B., Scranton R., Fukugita M., Richards G., 2010a, *MNRAS*, **405**, 1025
- Ménard B., Kilbinger M., Scranton R., 2010b, *MNRAS*, **406**, 1815
- Muller S., Wu S.-Y., Hsieh B.-C., González R. A., Loinard L., Yee H. K. C., Gladders M. D., 2008, *ApJ*, **680**, 975
- Oesch P. A., et al., 2014, *ApJ*, **786**, 108
- Peebles P. J. E., 1993, *Principles of Physical Cosmology*
- Planck Collaboration et al., 2014, *A&A*, **571**, A8
- Popping G., Somerville R. S., Galametz M., 2016, preprint, (arXiv:1609.08622)
- Reddy N. A., Steidel C. C., 2009, *ApJ*, **692**, 778
- Reichardt C. L., et al., 2009, *ApJ*, **694**, 1200
- Santini P., et al., 2010, *A&A*, **518**, L154
- Schiminovich D., et al., 2005, *ApJ*, **619**, L47
- Spergel D. N., et al., 2007, *ApJS*, **170**, 377
- Stognienko R., Henning T., Ossenkopf V., 1995, *A&A*, **296**, 797
- Vavryčuk V., 2017, *MNRAS*, **465**, 1532
- Watson D., Christensen L., Knudsen K. K., Richard J., Gallazzi A., Michałowski M. J., 2015, *Nature*, **519**, 327
- Wright E. L., 1981, *ApJ*, **250**, 1
- Wright E. L., 1982, *ApJ*, **255**, 401
- Wright E. L., 1987, *ApJ*, **320**, 818
- Wright E. L., 1991, *ApJ*, **375**, 608
- Xie X., Shen S., Shao Z., Yin J., 2015, *ApJ*, **802**, L16